

Effects of Dissipation Energy on Vibrational and Sound Energy Flow

N. Nakagawa, Y. Sekiguchi, A. Higashi, O. Mahrenholtz

Sound radiating from vibrating structures is known as structure-borne sound. The purpose of the present paper is to study the generating mechanism of structure-borne sound. The analytical model is a rectangular plate, a typical element of structures. The plate is excited at one point. Damping is taken into consideration by using a proportionally damped model or a dashpot model. The dynamic response of the plate is calculated by using the finite element method to obtain vibrational and sound energies. The vibrational and sound energy flow patterns, which are expressed by vector quantities of structural and sound intensities, are compared. The effects of the vibrational dissipation energy on the flow patterns of the sound energy are also investigated and two types of flow patterns (S- and M-type) are found.

1 Introduction

Recently, sound or noise radiated from vibrating structures has become a problem of great interest. Noise reduction has evolved as an essential design consideration. Most of the sound radiated from vibrating structures is known as structure-borne sound. There are many reports with studies on estimation of sound power or the distribution of sound pressure (Kojima, 1980; Uno Ingard, 1987; Maidanik, 1962; Tanaka, 1991). There are, however, only few reports on the sound generating mechanism. And the sound generating mechanism, i. e. the change from vibrational energy to sound energy, is not yet clarified. The purpose of the present study is to investigate sound generating mechanisms from the view point of both sound energy and vibrational energy. In this paper, the analytical model is a rectangular plate. The plate is excited sinusoidally at one point, because in this case vibrational energy flow patterns are obvious or simple. The dynamic response of the plate is calculated by using the finite element method to obtain vibrational energy and sound energy. Vibrational and sound energy flow are expressed by use of structural intensity (Noiseux, 1969; Pavic, 1976) and sound intensity (Mann, 1987), respectively. The sound field is analyzed in the near field of the vibrating plate where the vibrational energy of the plate is converted into sound energy. The present paper deals with the following: By changing the magnitude of damping, vibrational and sound energy are investigated by using three parameters which are sound radiation efficiency, energy ratio, and loss factor.

2 Vibrational Energy and Sound Energy

2.1 Vibrational Energy

The vibrational energy flow is expressed by the structural intensity, which is a vector quantity with components of magnitudes

$$W_x \text{ and } W_y \quad (1)$$

where W_x and W_y are structural intensity in the x - and y -direction, respectively. The structural intensity W_x is composed of three components which are the component of shear force, bending moment, and twisting moment, as given by equation (2).

$$W_x = j\omega B \left[w \frac{\partial}{\partial x} \left(\frac{\partial^2 w^*}{\partial x^2} + \frac{\partial^2 w^*}{\partial y^2} \right) - \frac{\partial w}{\partial x} \left(\frac{\partial^2 w^*}{\partial x^2} + \nu \frac{\partial^2 w^*}{\partial y^2} \right) - (1-\nu) \frac{\partial w}{\partial y} \frac{\partial^2 w^*}{\partial x \partial y} \right] \quad (2)$$

where w is the displacement of the plate, j is the unit of imaginary number, ω is the angular frequency, B is the bending stiffness of the plate, ν is Poisson's ratio, and $*$ denotes the complex conjugate number. The expressions in the y -direction are obtained by interchanging x with y in the equation (2). Structural intensity is calculated by using finite difference approximations. Here, the measuring points 1 to 8 for two-dimensional structural intensity are shown in Figure 1. The approximated equations for equation (2) are expressed as follows:

$$\begin{aligned}
 w &= \frac{1}{2}(w_3 + w_6) \\
 \frac{\partial w}{\partial x} &= \frac{1}{\Delta}(w_3 - w_6) \\
 \frac{\partial w}{\partial y} &= \frac{1}{4\Delta}(w_2 - w_4 + w_5 - w_7) \\
 \frac{\partial^2 w}{\partial x^2} &= \frac{1}{2\Delta^2}(w_1 - w_3 - w_6 + w_8) \\
 \frac{\partial^2 w}{\partial y^2} &= \frac{1}{2\Delta^2}(w_2 - 2w_3 + w_4 + w_5 - 2w_6 + w_7) \\
 \frac{\partial^2 w}{\partial x \partial y} &= \frac{1}{2\Delta^2}(w_2 - w_4 + w_5 - w_7) \\
 \frac{\partial}{\partial x} \left(\frac{\partial^2 w}{\partial x^2} + \frac{\partial^2 w}{\partial y^2} \right) &= \frac{1}{\Delta^3}(w_1 + w_2 - 5w_3 + w_4 - w_5 + 5w_6 - w_7 - w_8)
 \end{aligned}$$

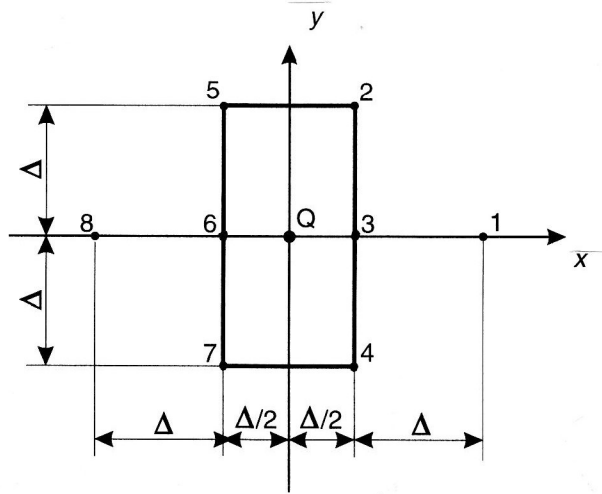


Figure 1. The Measuring Points for 2-dimensional Structural Intensity (x -direction)

2.2 Sound Energy

The sound energy flow is expressed by sound intensity which is given by a vector quantity. The coordinate system to calculate sound intensity is shown in Figure 2. The vibrating plate is divided into many elements, which are assumed to be vibrating in the same way as pistons. Sound intensity magnitude I at the measuring point $P(x, y, z)$ in Figure 2, is expressed by equation (3), because the sound intensity is contributed to all elements of the plate.

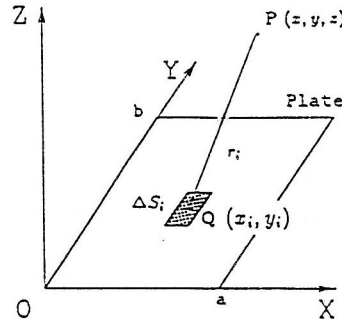


Figure 2. Coordinate System for Analysis of Sound Field

$$I = \frac{1}{2} \sum_{i=1}^N p_i \sum_{i=1}^N \bar{u}_i^* \quad (3)$$

where p_i is the sound pressure of the i th element, \bar{u}_i is the particle velocity of the i th element, and N is the number of the elements. The sound pressure p_i and the particle velocity in the x , y , z -direction u_{xi} , u_{yi} , u_{zi} are given by equations (4) to (5c), respectively.

$$p_i = j\omega\rho \frac{A_i}{r_i} \exp j(\omega t - \kappa r_i) \quad (4)$$

$$u_{xi} = A_i (x - x_i) r_i^{-2} (r_i^{-1} + j\kappa) \exp j(\omega t - \kappa r_i) \quad (5a)$$

$$u_{yi} = A_i (y - y_i) r_i^{-2} (r_i^{-1} + j\kappa) \exp j(\omega t - \kappa r_i) \quad (5b)$$

$$u_{zi} = A_i z r_i^{-2} (r_i^{-1} + j\kappa) \exp j(\omega t - \kappa r_i) \quad (5c)$$

where A_i , r_i , κ are as follows:

$$A_i = j\omega\rho(x_i, y_i)\Delta S_i / 2\pi$$

$$r_i = \sqrt{(x - x_i)^2 + (y - y_i)^2 + z^2}$$

$$\kappa = \omega / c = 2\pi z / \lambda$$

The quantities x_i and y_i are positions of the i th element, ρ is the air density, c is the sound velocity and ΔS_i is the area of the i th element. As the measuring height z of sound intensity influences the sound intensity, the non-dimensional parameter μ given by equation (6) is used, so that the measuring height becomes similar for all frequencies.

$$\mu = \kappa z \quad (6)$$

3 Analysis and Results

3.1 Analysis of Vibrating Plate

The analytical model is shown in Figure 3. The surroundings of the plate are fixed, and it is assumed that the plate is sufficiently thin to be analyzed as a thin plate. The plate is excited sinusoidally at point A shown in Figure 3, and the material constants for analysis of the plate are shown in Table 1.

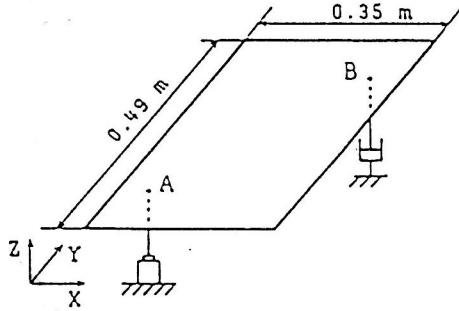


Plate thickness	m	1.50×10^{-3}
Young's modulus	Pa	2.06×10^{11}
Mass density	kg/m ³	7.85×10^3
Poisson's ratio		0.30

Table 1. Material Constants

Figure 3. Analytical Model

The vibrating plate is analyzed by using the finite element method. The equation of motion is expressed by equation (7).

$$[M]\{\ddot{w}\} + [C]\{\dot{w}\} + [K]\{w\} = \{f\} \quad (7)$$

where $[M]$, $[C]$ and $[K]$ are mass, damping and stiffness matrix of the plate, respectively, $\{w\}$ is the displacement vector and $\{f\}$ is the force vector. The damping matrix $[C]$ is given by the proportional damping expressed by equation (8).

$$[C] = \alpha[M] + \beta[K] \quad (8)$$

where α and β are proportional damping coefficients. When the modal damping ratio is used, the modal damping ratio ζ_{mn} of the (m, n) mode is expressed by equation (9).

$$\zeta_{mn} = \frac{1}{2} \left(\frac{\alpha}{\Omega_{mn}} + \beta \Omega_{mn} \right) \quad (9)$$

where Ω_{mn} is the undamped natural angular frequency of the (m, n) mode. In this paper, damping is taken into consideration by using both a proportionally damped model and a dashpot model, i.e. the modal damping ratio ζ_{mn} is used for the dashpot model.

Analysis is performed for the 1st mode to the 10th mode. As typical examples only the analytical results for the 2nd mode ((1,2) mode) and 5th mode ((2,2) mode) are shown in this paper, because analytical results of all modes have **similar** tendencies. The mode shapes of the (1,2) mode and the (2,2) mode are shown in Figure 4.

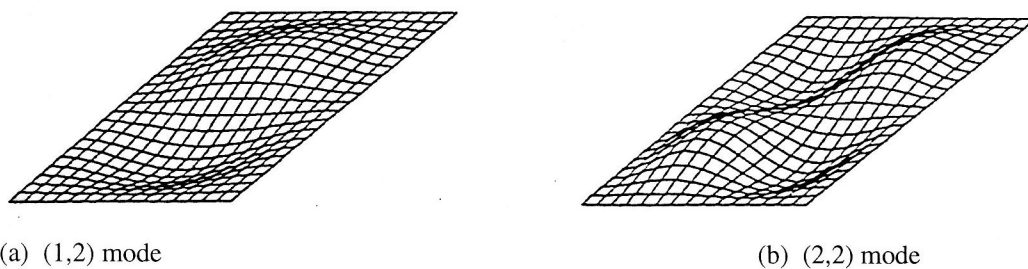


Figure 4. Mode Shape

3.2 Distribution of Structural Intensity and Sound Intensity

When the excitation is forced sinusoidally at point A in Figure 3, vibrational and sound energy on the plate are analyzed. The magnitude of the excitation force is constant. The effects of dissipation energy of the plate on vibrational and sound energy are investigated by using the modal damping ratio or the damping coefficient. Here, although the structural intensity vector is assumed to be a 2-dimensional quantity, the sound intensity vector is a 3-dimensional quantity. In this paper, to compare the structural intensity vector with the sound intensity vector, the sound intensity vector is in the 2 dimensions of x and y . The length of the vector is normalized, so that vibrational energy and sound energy are converted into dB. The analytical results are shown in Figure 5, when vibrational energy is equally dissipated in the plate. Figure 6 shows the analytical results, when vibrational energy is dissipated by the damper at point B. It is found that the sound intensity vector map changes when the dissipation energy is increased. The flow pattern of the radiated sound energy (Figures 5, 6(a)) can be estimated as vibrational mode shape (Figure 4(b)), when the dissipation energy is small. On the other hand when the dissipation energy is enlarged, the flow pattern of the radiated sound energy (Figures 5, 6(b)) is similar to the vibrational energy flow pattern. But the structural intensity vector map is not changed in spite of the increase of dissipation energy. It was found that the other vibration modes have similar tendencies and that consequently the radiated sound energy flow has two types of flow patterns. In this study, the sound energy flow pattern depending on the vibration mode is called M-type, and the sound energy flow pattern similar to the vibrational energy flow is called S-type.

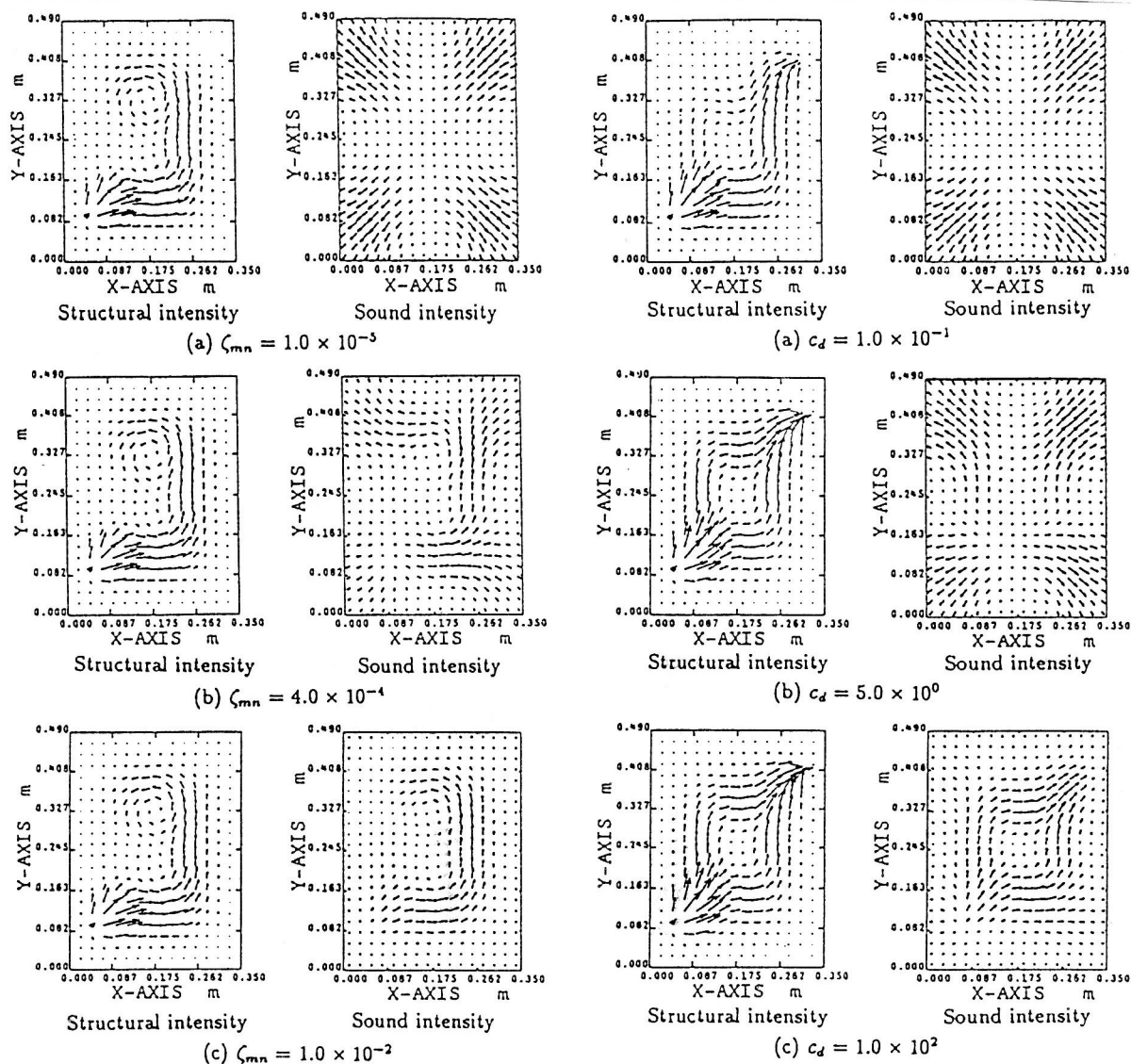


Figure 5. Structural Intensity and Sound Intensity Vector Map ((2,2) mode, ζ_{mn} = Modal Damping Ratio)

Figure 6. Structural Intensity and Sound Intensity Vector Map ((2,2) mode, c_d = Damping Coefficient)

3.3 Energy Flow from Structural Vibration to Sound

The energy flow from excitation of the plate to sound radiation in the condition of steady vibration is schematically shown in Figure 7. In this figure, E_1 to E_6 are the input energy (exciting energy), the vibrational energy of the plate, the vibrational energy of the surrounding air, the propagated sound energy, the dissipation energy of the plate and the unpropagated sound energy. The alteration of energies E_1 to E_4 relating to the two kinds of damping is shown in Figures 8 and 9. When the modal damping ratio and the damping coefficient are enlarged, all energies are decreased, with the input energy E_1 at a smaller rate than the other energies.

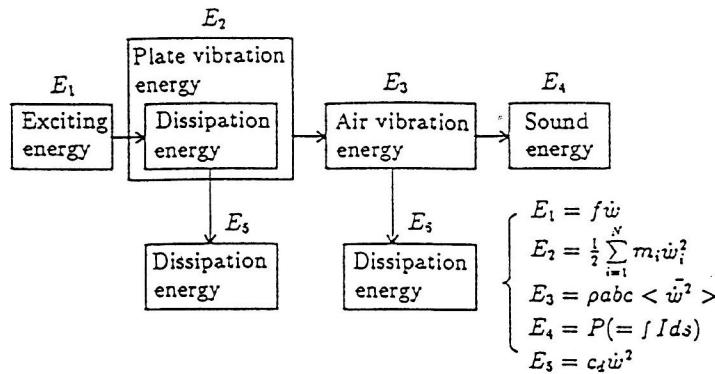


Figure 7. Energy Flow about Generation of Structure-borne Sound

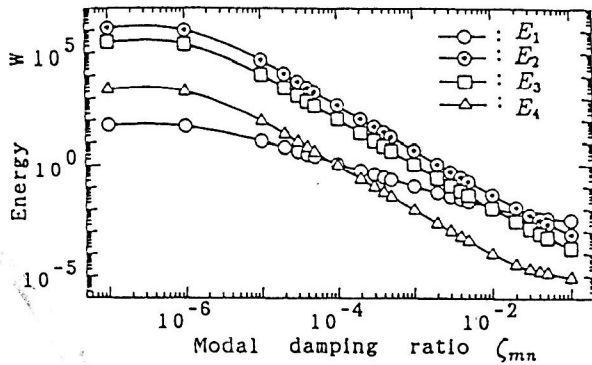


Figure 8. Relationship between Modal Damping Ratio and Vibrational and Sound Energies ((2,2)mode)

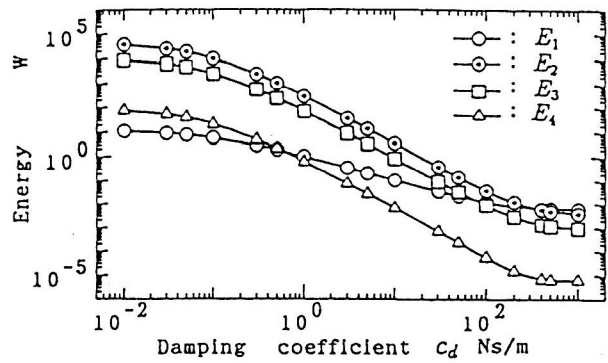


Figure 9. Relationship between Damping Coefficient and Vibrational and Sound Energies ((2,2)mode)

4 Relationship between Dissipation Energy and Sound Field

M- and S-types of the sound energy flow pattern are compared by using three parameters, viz. sound radiation efficiency, energy ratio, and loss factor.

4.1 Sound Radiation Efficiency

Sound radiation efficiency, which is calculated by the sound power radiated from the vibrating structure, is expressed by equation (10).

$$\sigma = \frac{P}{pabc \langle \bar{v}^2 \rangle} \quad (10)$$

and where P and $\langle \bar{v}^2 \rangle$ are sound power and the time and spatial average of the plate vibration velocity, respectively, and a and b are plate side lengths. The calculated results of sound radiation efficiency are shown in Figures 10 and 11. It is found, in Figure 10, that the value of sound radiation efficiency is constant in the area $\zeta_{mn} \leq 1.0 \times 10^2$ and that the sound energy flow pattern of M- and S-types is mixed in this area. Next, when the sound radiation efficiency is constant or is not, the mode shapes are shown in Figure 12. As a result, the mode shape is found to be obvious in the case that sound radiation efficiency is constant. Sound radiation efficiency does change, when the vibrational mode shape is modified. Therefore sound radiation efficiency is found to be decided by the mode shape, and not by the dissipation energy. Consequently sound radiation efficiency is found to be a parameter which is not able to classify the sound energy flow patterns (i.e. M- and S-types).

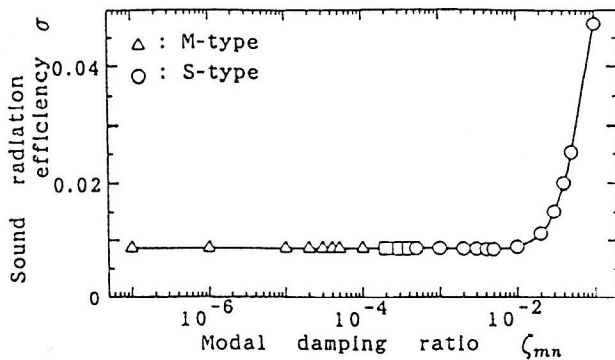


Figure 10. Relationship between Modal Damping Ratio and Sound Radiation Ratio ((2,2)mode)

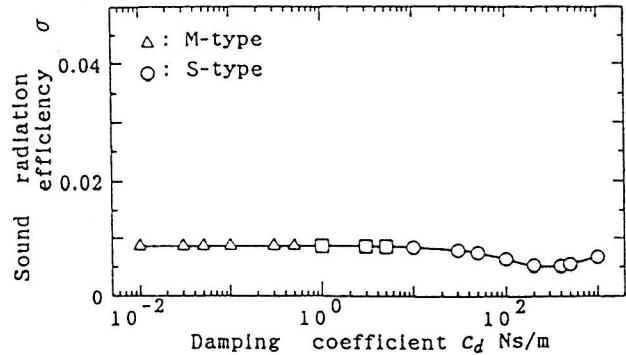
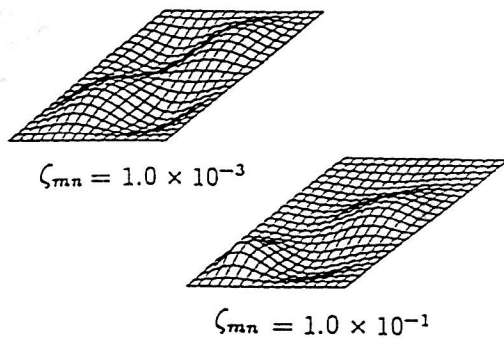
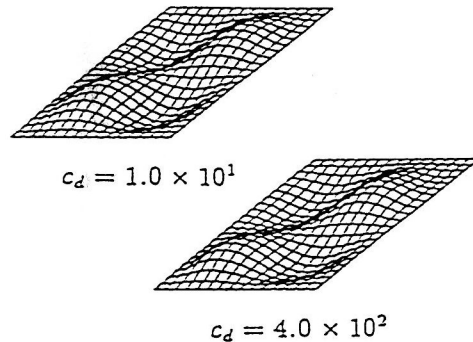


Figure 11. Relationship between Damping Coefficient and Sound Radiation Ratio ((2,2)mode)



(a) Modal Damping Ratio ζ_{mn}



(b) Damping coefficient c_d

Figure 12. Change of Mode Shape for Damping Effect ((2,2)mode)

4.2 Proposal of Energy Ratio

Dissipation energy is equal to input energy of the vibrating plate under the condition of steady vibration. Therefore, it can be considered that the dissipation energy is equal to the propagated vibrational energy from the exciting point to the damping point, which is obtained by integrating the structural intensity over a circumference around the exciting point. Here, we consider an energy ratio η_{si} which is defined by the ratio of sound energy to dissipation energy. The energy ratio η_{si} is expressed by equation (11).

$$\eta_{si} = \frac{E_s}{E_i} \quad (11)$$

where E_s and E_i are sound energy and dissipation energy, respectively. This parameter is found to express the comparison of the mechanical energy in the plate with the propagating sound energy in space. The calculated results of this parameter are shown in Figures 13 and 14. Here, the results of the (2,2)mode and the (1,2)mode are shown for comparison with other vibrational modes. In these figure, the symbols Δ and \blacktriangle indicate the sound energy flow pattern of M-Type, the symbols \circ and \bullet indicate the sound energy flow pattern of S-type, and the symbols \square and \blacksquare indicate the transient flow pattern composed of M-type and S-type, respectively. These figures show that these energy flow patterns are clearly divided by the energy ratio. That is, these sound energy flow patterns are found to indicate that M-type flow patterns appear in the area of $\eta_{si} \geq 1.0$, and S-type flow patterns appear in the area of $\eta_{si} \leq 0.1$.

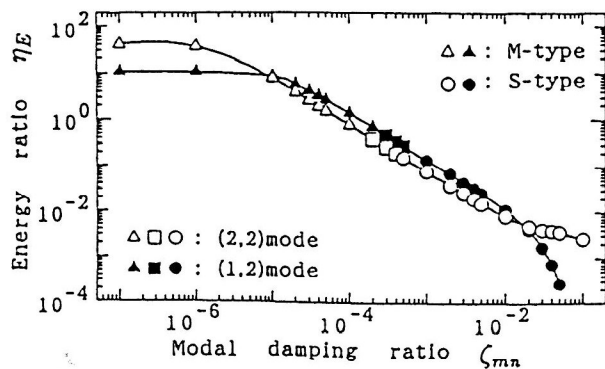


Figure 13. Relationship between Modal Damping Ratio and Energy Ratio ((2,2) and (1,2)mode)

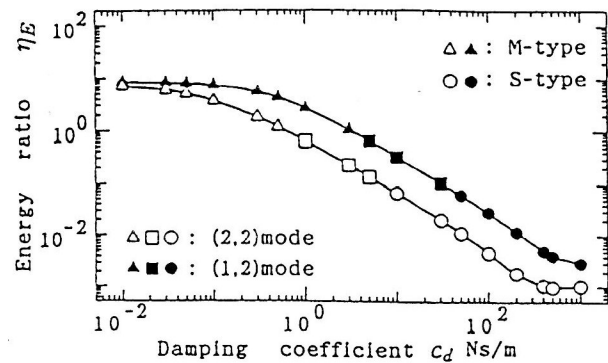


Figure 14. Relationship between Damping Coefficient and Energy Ratio ((2,2) and (1,2)mode)

4.3 Loss Factor

In this paragraph, the sound energy flow patterns are investigated by using the loss factor which is calculated by the half-bandwidth method. Figures 15 and 16 which indicate the calculated results, show the comparison of the (2,2)mode with (1,2)mode for reference. In these figures, the symbols are similar to those in Figures 10 and 11, but the symbols \bullet , \blacksquare and \blacktriangle indicate the results calculated by using the modal damping ratio and the symbols \circ , \square and Δ indicate the results calculated by using the damping coefficient. The relationship between the energy ratio and the loss factor is found to be coincident for the two kinds of damping for each mode. Classification of the sound energy flow pattern is possible by using the loss factor for each mode. Furthermore the energy ratio is able to classify into M- and S-types for all modes regardless of the damping involved.

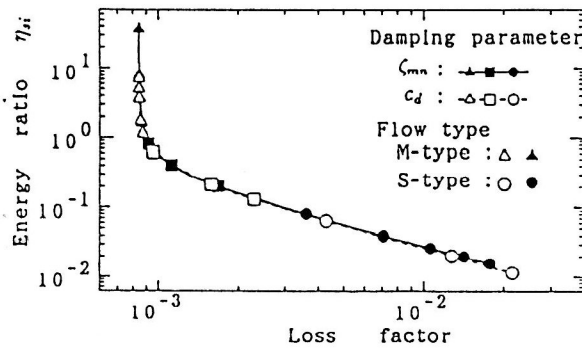


Figure 15. Relationship between Loss Factor and Energy Ratio ((2,2)mode)

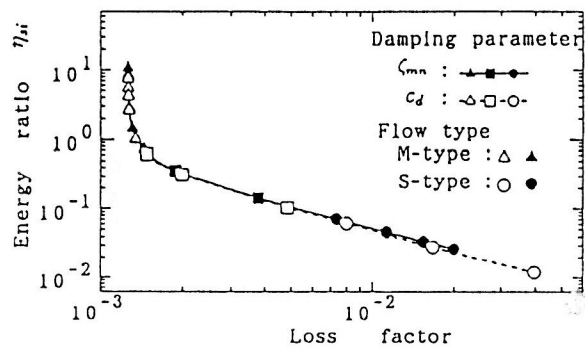


Figure 16. Relationship between Loss Factor and Energy Ratio ((1,2)mode)

5 Conclusions

In this paper we investigated the effects of dissipation energy on the vibrational and the sound energy flow. The main results obtained are as follows:

- (1) The flow pattern of the radiated sound intensity showed the existence of two types, viz. the flow pattern called M-type dependent on the vibration mode, and the flow pattern called S-type similar to the vibrational energy flow pattern.
- (2) The flow pattern of the radiated sound energy of S- and M-types can be classified by the energy ratio η_{si} . That is,

$$\begin{aligned} &\text{for } \eta_{si} \geq 1.0 : \text{M-type} \\ &\text{for } \eta_{si} \leq 0.1 : \text{S-type} \\ &\text{for } 0.1 \leq \eta_{si} \leq 1.0 : \text{transient region from M-type to S-type} \end{aligned}$$

- (3) From the result obtained for the three kinds of parameter (i.e. sound radiation efficiency, energy ratio, and loss factor), it was found that only the energy ratio is able to classify the sound energy flow into the patterns of M-type and S-type.
- (4) Sound radiation efficiency is dependent on the mode shape regardless of the magnitude of the dissipation energy.

Literature

1. Kojima, N.; Ikoma, K.; Fukuda, M.: Trans.Jpn.Mech.Eng., 46-411 C (1980), 1355 (in Japanese).
2. Maidanik, G.: Response of Ribbed Panels to Reverberant Acoustic Fields, J. Acoust. Soc. Am., 34 (1962), 809.
3. Mann, J. A.; Tichy, I. J.; Romano, A. J.: Instantaneous and time-averaged energy transfer in acoustic fields, J. Acoust. Soc. Am., 82 (1987), 17.

4. Noiseux, D. U.: Measurement of Power Flow in Uniform Beams and Plates, *J. Acoust. Soc. Am.*, 47 (1969), 238-247.
5. Pavic, G.: Measurement of Structure Borne Wave Intensity (Part 1: Formulation of the Methods), *J. Sound Vib.*, 49-2 (1976), 221-230.
6. Tanaka, N.; Kikushima, Y.; Kuroda, M.: Active Control of the Structure-borne Sound (On the Relationship between the Control Effect of Vibration and the Sound), *Trans. Jpn. Mech. Eng.*, 57-537 C (1991), 1512 (in Japanese).
7. Uno Ingard, K.; Akay, A.: Acoustic Radiation From Bending Wave of a Plate, *Trans. ASME.*, 109 (1987), 75.
8. Wallace, C. E.: Radiation Resistance of a Rectangular Plate, *J. Acoust. Soc. Am.*, 51 (1972), 946.

Addresses: Professors Noritoshi Nakagawa and Yasuhisa Sekiguchi, Hiroshima University, Cluster I (Mechanical Engineering), 1-4-1 Kagamiyama, Higashi-Hiroshima 739, Japan; Akihiko Higashi, Graduate School of Hiroshima University; Professor Oskar Mahrenholtz, Meerestechnik II, Technische Universität Hamburg-Harburg, Eißendorfer Straße 42, D-21073 Hamburg.